doi:10.1016/j.jmb.2005.05.020 J. Mol. Biol. (2005) 350, 735–743

JMB

Available online at www.sciencedirect.com

SCIENCE DIRECT®

ELSEVIER

# Crystal Structure of a CRISP Family $Ca^{2+}$-channel Blocker Derived from Snake Venom

**Yasuo Shikamoto[1], Kyoko Suto[1], Yasuo Yamazaki[2], Takashi Morita[2]* and Hiroshi Mizuno[1]***

[1]*Department of Biochemistry National Institute of Agrobiological Sciences Kannondai 2-1-2, Tsukuba Ibaraki 305-8602, Japan*

[2]*Department of Biochemistry Meiji Pharmaceutical University, Kiyose, Tokyo 204-8588, Japan*

**Corresponding author*

The cysteine-rich secretory proteins (CRISPs) are widely distributed in mammals, reptiles, amphibians and secernenteas, and are involved in a variety of biological reactions. Here we report the crystal structure of triflin, a snake venom derived blocker of high $K^+$-induced artery contraction, at 2.4 Å resolution. Triflin consists of two domains. The first 163 residues form a large globular body with an α–β–α sandwich core, which resembles pathogenesis-related proteins of group-1 (PR-1). Two glutamic acid-associated histidine residues are located in an elongated cleft. A $Cd^{2+}$ resides in this binding site, and forms a five-coordination sphere. The subsequent cysteine-rich domain adopts a rod-like shape, which is stabilized by five disulfide bridges. Hydrophobic residues, which may obstruct the target ion-channel, are exposed to the solvent. A concave surface, which is surrounded by these two domains, is also expected to play a significant role in the binding to the target receptor, leading to ion channel blockage. The C-terminal cysteine-rich region has a similar tertiary structure to voltage-gated potassium channel blocker toxins, such as BgK and ShK. These findings will contribute toward understanding the functions of the widely distributed CRISP family proteins.



*Keywords:* CRISP; trifling; crystal structure; $Ca^{2+}$ channel blocker; snake venom

## Introduction

Cysteine-rich secretory proteins (CRISPs) are single chain polypeptides with molecular masses of 20–30 kDa. The CRISPs are found in a variety of organisms, such as mammals, reptiles, amphibians and secernenteas. Acidic epididymis glycoprotein (AEG, also known as protein D/E or CRISP-1), the first discovered CRISP, was isolated from mammalian epididymis. AEG is an androgen-regulated secretory protein, which may be involved in gamete fusion.[1–3] Two other mammalian CRISPs have been isolated and characterized: CRISP-2 (testis-specific protein 1; TPX-1)[4] and CRISP-3 (specific granule protein of 28 kDa; SGP28).[5] Although CRISP-3 is a specific ligand for plasma $\alpha_1$β-glycoprotein (A1BG), very little clear evidence exists for the physiological function of either protein. In addition to the aforementioned mammalian CRISPs, a variety of other CRISP family proteins have been found, and their molecular functions have been characterized. For example, helothermine, from the venom of the Mexican beaded lizard (*Heloderma horridum horridum*), modulates a variety of ion channels, including voltage-gated calcium channels, voltage-gated potassium channels, and ryanodine receptors.[6–9] Recently, allurin from *Xenopus* egg jelly was shown to act as a sperm chemoattractant.[10] In addition, SCL-1, whose expression is controlled by the transcription factor DAF-16, was shown to positively regulate longevity and stress resistance in *Caenorhabditis elegans*.[11] Thus, CRISPs exist in several organisms and exhibit diverse biological functions. Although these CRISPs are derived from various origins, they share high amino acid sequence similarity. In particular, all 16 cysteine residues are strictly conserved, and remarkably, ten of these are clustered in the C-terminal third of each protein. The CRISPs are expected to exhibit two

Present address: Y. Shikamoto, K. Suto, and H. Mizuno, VALWAY Technology Center, NEC Soft Co. Ltd, Shinkiba 1-18-6, Kotoku, Tokyo 136-8608, Japan.

Abbreviations used: CRISP, cysteine-rich secretory protein; PR-1, pathogenesis-related proteins of group 1; Pdc, pseudecin; PsTx, pseudechetoxin.

E-mail addresses of the corresponding authors: tmorita@my-pharm.ac.jp; mizuno-hiroshi@aist.go.jp

domain-like structures, based on comparisons to other proteins with similar amino acid sequences. The N-terminal domain is composed of ~160 residues, and exhibits high homology with the group 1 plant pathogenesis-related proteins (PR-1) and the insect venom antigen 5 proteins (Ag 5), which are involved in plant stress-resistance and venom allergens, respectively. The other consists of the region following the PR-1 protein homologous sequence, which forms a cysteine-rich domain. The structures of the PR-1 protein from tomato (P14a) and the antigen 5 protein from hornet venom (Ves v 5) have been defined by an NMR solution analysis[12] and an X-ray crystallographic study,[13] respectively, which revealed their similar tertiary structures. Thus, structural information about the N-terminal domains of these proteins is available, but the structure of the C-terminal cysteine-rich domain is still poorly understood.

Recently, we have identified and cloned several CRISPs from snake venoms.[14,15] These snake venom CRISPs share high amino acid sequence identity with the mammalian CRISPs (~50% identity *versus* AEG), and all of the cysteine residues are completely conserved. Triflin, a CRISP isolated from the venom of the Habu snake (*Trimeresurus flavoviridis*), blocks smooth muscle contraction, which might be caused by the inhibition of an L-type $Ca^{2+}$ channel, like the activities of ablomin and latisemin from other snake venoms.[16] Pseudechetoxin (PsTx) and pseudecin (Pdc), which are CRISPs from the venoms of the Australian king brown snake (*Pseudechis australis*) and the red-bellied black snake (*Pseudechis porphyriacus*), respectively, block cyclic nucleotide-gated ion (CNG) channels by contacting the pore turret region of the channel and inhibiting ion entry at the extracellular side of the channel.[17–19] The amino acid sequences of these snake venom CRISPs are homologous to each other, but the targets of the proteins are different. Previous studies revealed that the residues responsible for the selectivity reside within the cysteine-rich region.[16] However, the details of the inhibition mechanism are unclear, due to the lack of structural information.

Here we describe the crystal structure of triflin, a CRISP from snake venom. This structural information about triflin will provide novel insights into the structure–function relationships of the CRISP family proteins.

## Results and Discussion

### Crystal structure determination

Native crystals of triflin were grown by vapor diffusion in hanging drops, and diffracted X-rays to 2.4 Å resolution. We obtained an electron density map using the multiwavelength anomalous scattering of gold in a single derivative crystal, as described in Materials and Methods. After the density modification, the initial electron density map allowed the tracing of most of the molecule. In the gold derivative structure, two gold atoms were observed, which were chelated by histidine residues. The gold atoms were replaced by cadmium ions in the native structure. The final model comprises a triflin molecule, nine cadmium ions, two acetic acid molecules, and 148 water

**Table 1.** Data collection, phasing and refinement statistics

| | Native | Peak | Edge | Remote |
|---|---|---|---|---|
| Data collection | | | | |
| Wavelength (Å) | 1.0403 | 1.0403 | 1.0406 | 1.0457 |
| Resolution range (Å) | 40–2.4 (2.5–2.4) | 50–2.5 (2.6–2.5) | 50–2.5 (2.6–2.5) | 50–2.6(2.7–2.6) |
| Space group | $P4_32_12$ | $P4_32_12$ | | |
| Unit cell parameters (Å) | | | | |
| *a*, *b* | 83.87 | 83.20 | 83.35 | 83.33 |
| *c* | 85.68 | 85.61 | 85.96 | 85.99 |
| Unique reflections | 13,969 | 10,644 | 10,732 | 10,940 |
| Observed reflections | 250,751 | 80,896 | 82,831 | 91,738 |
| Completeness (%) | 99.4 (99.4) | 98.2 (98.2) | 98.2 (98.2) | 99.4 (99.4) |
| $R_{sym}$ | 0.063 (0.303) | 0.061 (0.392) | 0.060 (0.446) | 0.077 (0.535) |
| $\langle I\rangle/\langle\sigma I\rangle$ | 8.2 (2.5) | 7.7 (7.1) | 7.7 (6.9) | 8.4 (7.6) |
| Phasing | | | | |
| Phasing power isomorphous (acentric/centric) | | 0.574/.482 | 1.589/1.534 | –/– |
| Phasing power anomalous (acentric/centric) | | 1.120/– | 1.237/– | 0.476/– |
| $R_{Cullis}$ isomorphous (acentric/centric) | | 0.668/0.675 | 0.561/0/495 | –/– |
| $R_{Cullis}$ anomalous (acentric/centric) | | 0.716/– | 0.749/– | 0.875/– |
| FOM (acentric/centric) | | 0.400/0.251 | | |
| Refinement | | | | |
| $R_{work}/R_{free}$ (%) | 22.6/28.2 | | | |
| rmsd bonds | 0.0059 | | | |
| rmsd angles | 1.16 | | | |
| No. of atoms (protein/water) | 1733/140 | | | |
| *B* (Å$^2$) (protein/water) | 55.6/59.9 | | | |
| Ramachandran plot (%) | | | | |
| Most favored | 81.8 | | | |
| Allowed | 18.2 | | | |
| Disallowed | 0.0 | | | |

molecules. The final $R_{work}$ and $R_{free}$ values are 0.225 and 0.284 at 2.4 Å resolution, respectively (Table 1).

### Overview of the triflin crystal structure

The triflin structure (Figure 1(a)) consists of two domains. Briefly, 163 residues from the N terminus compose a globular body with an α–β–α sandwich core, with a structure similar to those of the PR-1 proteins. So far, only two PR-1 protein structures have been reported. One is an NMR solution structure of P14a (Figure 1(b)),[12] whose expression is induced by stress stimulation. The other is the crystal structure of the antigen 5 protein, termed Ves v 5, which is a component of the venom of yellow hornet (Figure 1(c)).[13] A conspicuous feature of the triflin structure is the subsequent cysteine-rich domain, which forms a rod-like shape, and a concave surface is observed between these domains. A comparison of the triflin structure with those of P14a and Ves v 5 yields rmsd values of 1.43 Å and 1.03 Å, respectively. In the triflin structure, the first 11 residues of the N-terminal peptide chain (Asn1-Lys 11), which are absent from the other two proteins, contribute toward forming the first helix. In addition to the N-terminal helix, inserted residues (Pro31-Asn35 and Asp64-Cys73) form two strands (β1 and β3) and one helix (α4). Thus, the structure of the triflin PR-1 domain is similar, but somewhat bulky, as compared to those of P14a and Ves v 5.

### Cysteine-rich domain of triflin

The C-terminal cysteine-rich domain, with five well-conserved disulfide bridges (Cys167-Cys174, Cys170-Cys179, Cys183-Cys216, Cys192-Cys210, and Cys201-Cys214 shown in Figure 2), may begin at Cys167 for the following two reasons. (1) The C terminus of Ves v 5, which lacks the cysteine-rich domain, resides at Lys164, and (2) the conserved residues Gly-Pro-Pro, just before Cys167, may form

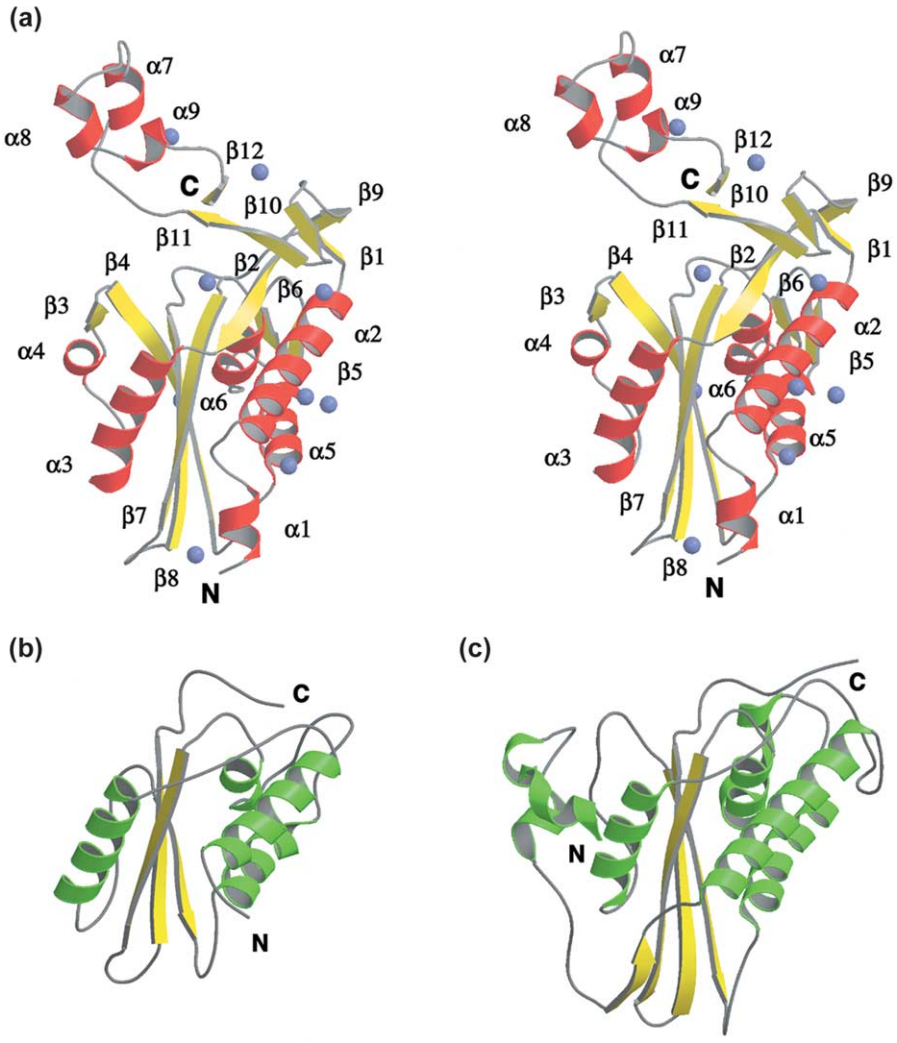


**Figure 1.** Comparison of the structures of triflin, P14a, and Ves v 5. Ribbon model of main chain of triflin, drawn as a stereo pair (a). Helices and strands are shown in red and yellow, respectively. Cd ions are shown as blue spheres. Ribbon models of P14a (b) and Ves v 5 (c) drawn from the same viewpoint, with helices in green and strands in yellow.

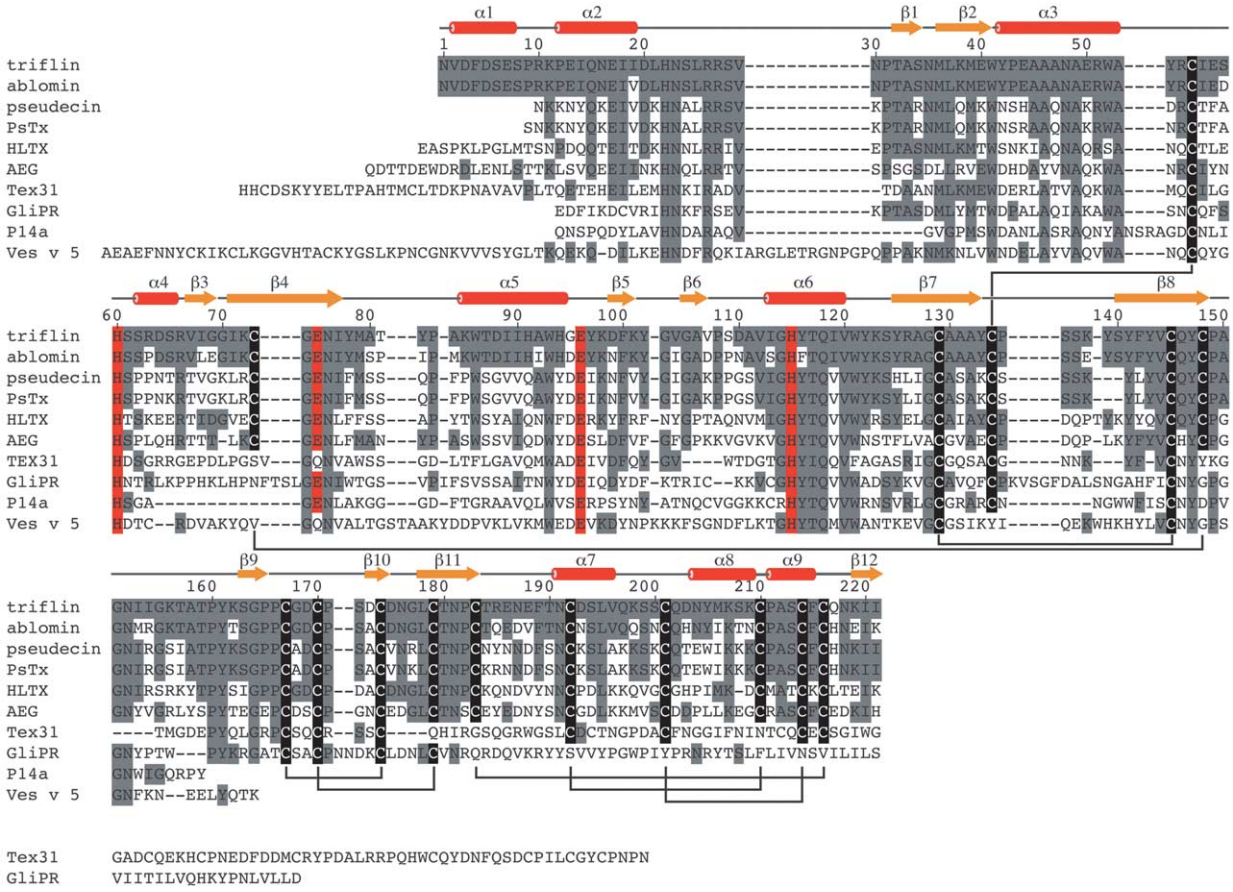


**Figure 2.** Sequence alignment of the CRISP and PR-1 proteins. The identical residues are shadowed in grey, and the residues involved in the $Cd^{2+}$ coordination are highlighted in red columns. All cysteine residues are reversed characters. Gaps (−) were inserted to maximize similarity. Cysteine residues that form disulfide bonds in the cysteine-rich domain are connected by continuous lines. The locations of the regular secondary structure elements identified for triflin are depicted at the top, with the α-helices and β-strands highlighted by red columns and yellow arrows, respectively. The numbering for triflin is indicated above its sequence.

a linker chain between the two domains. The cysteine-rich domain has an unusually elongated shape that spans about 38 Å, and it appears to be divided into two sub-domains. The N-terminal sub-domain (Cys167 to Cys179) forms a compact fold with two disulfide bridges and two antiparallel β strands (β10) and β11). The β11 in the cysteine-rich region and β2 in the PR-1 domain are anchored by two hydrogen bonds involving backbone chain atoms. Thus, the N-terminal sub-domain appears to be part of the PR-1 domain. The C-terminal sub-domain (42 amino acid residues) contains three short helices and appears to be stabilized by three disulfide bridges. It begins at Thr180 in the middle of the β11 strand, and ends at a short β strand (β12) that interacts with β11 through two main-chain hydrogen bonds. This fold is different from those found in the voltage-sensor toxins from other venoms[20,21] which inhibit ion channels. Those voltage-sensor toxins are small disulfide core proteins (about 35 amino acid residues) with a hydrophobic face in one side, which may be important for voltage sensor inhibition.[22] With regard to the voltage-sensor toxins, the C-terminal sub-domain of triflin is similar, but slightly larger in size, and it has some solvent-exposed hydrophobic residues that might be important for receptor recognition, as described later. This suggests that the C-terminal sub-domain itself has functional activity. In terms of this connection, it is interesting that the C-terminal sub-domain does not interact with either the PR-1 domain or the N-terminal sub-domain, except that the C-terminal carboxyl group interacts with the side-chains of Tyr122 and Lys123, suggesting that the C-terminal sub-domain can move independently relative to the rest of the molecule. Rotations around certain covalent bonds in the backbone chain from Cys179 to Asn181 in the β11 strand might cause domain movement, as proposed on the basis of crystallographic evidence,[23] and the interactions involving the C-terminal carboxyl group are maintained because they are located in the proximity of the rotation axis. For example, the rotation around the $C^{\alpha}$–C bond of Cys179 is concerned directly with the opening and closing of the concave surface surrounded by the PR-1 domain and the C-terminal sub-domain.

### Putative triflin metal-binding site

During the process of searching for crystallization conditions, triflin crystals showed a tendency to appear in $Cd^{2+}$ containing solutions. After the structure analysis, nine $Cd^{2+}$ were observed in the asymmetric unit. Of these, seven $Cd^{2+}$ were coordinated with acidic residues (Glu or Asp), while two $Cd^{2+}$ were coordinated with histidine residues. One of these $Cd^{2+}$ is located in a putative metal-binding site formed by conserved histidine residues, as shown in Figure 3. His60 and His115 form a five-coordination sphere together with three water molecules. The $N^{\delta}$ atoms of His60 and His115 hydrogen bond to the carboxyl oxygen atoms of Glu75 and Glu96, respectively. The latter hydrogen bonding distance is 2.59 Å. Such a short hydrogen bond is also observed in the corresponding hydrogen bond in Ves v 5.[13] These histidine and glutamic acid clusters are strictly conserved in the CRISP and PR-1 family proteins, although Glu75 is substituted with glutamine in Tex31 and Ves v 5 (Figure 2), and they form a putative active site in the cleft, as shown in Figure 3(a). The corresponding site in P14a had been predicted as a putative $Zn^{2+}$ binding motif.[12,24] In the 20 deposited NMR structures of P14a, the $C^{\alpha}$ atoms of the histidine and glutamic acid residues are also located at similar positions as in triflin, although no metal ions were observed. The His93 side-chain (His115 in triflin) projects toward the cleft, as in the case of triflin; however, the His48 side-chain (His60 in triflin) has various orientations in the NMR models, which might be due to a lack of metal ions. A similar motif was observed in the Ves v 5 structure,[13] where both histidine residues pointed toward the center of the cleft. The site is capable of capturing heavy metals such as Hg and Pt ions, although no metal ion was reported in the native structure. This site is now confirmed as the putative

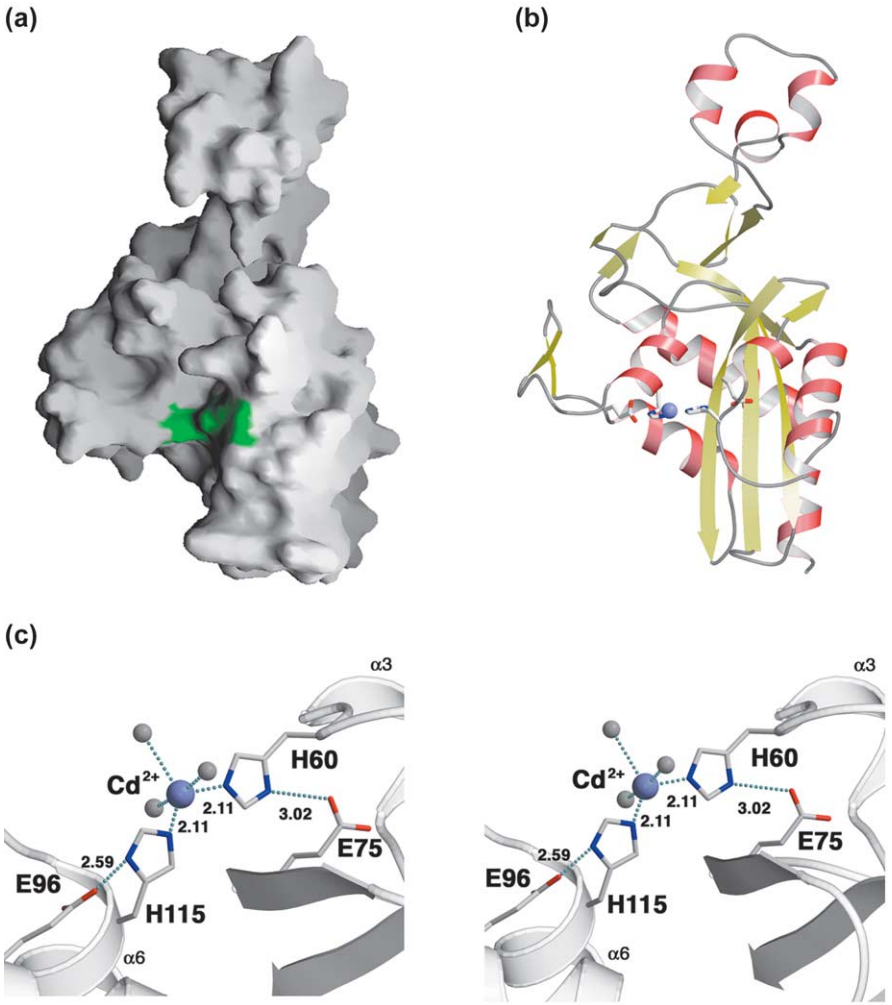


**Figure 3.** Triflin $Cd^{2+}$ binding site. (a) The $Cd^{2+}$ binding site is shown in green on the surface model. (b) The same view as in (a), but the entire model is shown in a ribbon presentation, with the clusters of histidine and aspartic acid residues and the $Cd^{2+}$ depicted by stick models and a blue sphere, respectively. (c) A close-up view of the $Cd^{2+}$-binding site, shown from a different direction. The three small grey spheres are water molecules that coordinate with the $Cd^{2+}$. Coordinations and hydrogen bonds are represented by broken lines, and their distances are indicated (Å).

active site in which the $Cd^{2+}$ was bound. This site *in vivo* could catch a $Zn^{2+}$ in place of the $Cd^{2+}$ observed in the present structure.

Recently, Tex31 was isolated and cloned from the venom duct of *Conus textile*, and was found to have the ability to cleave peptides.[25] Tex31 also shares sequence homology with the PR-1 proteins (Figure 2), although its C terminus has around 50 extra residues. Tex31 has proteolytic activity, which might contribute toward producing mature conotoxin peptides. The processing activity is increased by fivefold by the addition of $Ca^{2+}$, but decreased to 60% by the addition of EDTA or EGTA. These results suggested that Tex31 protein may be a metalloprotease, although serine protease inhibitors also suppressed the activity. Interestingly, His60, His115, Glu75 and Glu96 in triflin are conserved in Tex31 (Figure 2) even though one glutamic acid is replaced by glutamine. Unlike the metalloprotease family proteins, only two histidine residues coordinate with the metal ion, and no catalytic glutamate has been identified. Thus, the glutamic acid-associated histidine residues conserved in the CRISP family venom proteins are expected to function differently from those of the classic metalloprotease family proteins.

### Triflin active site for the inhibition of depolarization-induced muscle contraction

PsTx and Pdc of the venom CRISP family proteins have been well characterized in terms of the relationships with their target ion channels,[17–19] as compared with triflin. However, the three-dimensional structures of PsTx and Pdc have not been solved. The inhibitory active sites of PsTx and Pdc, as well as those of other proteins, can be discussed based on the structure of triflin, for the following reason. Triflin, PsTx and Pdc share highly homologous amino acid sequences, and the amino acid sequences of their target receptors are also similar to each other, indicating that the binding manner of triflin to the L-type $Ca^{2+}$ channel (considered to be the target receptors as described later) resembles those of PsTx and Pdc to the CNG channel. In excited outside-out patches containing CNG channels in the visual and olfactory systems, PsTx showed high affinity contacts with the pore turret of the CNG channel, suggesting that PsTx occludes the entrance to the pore.[19] This result was supported by subsequent studies, which revealed that the inhibitory affinity of PsTx was dramatically decreased by the mutations of residues on the turret region of the CNGA2 channel.[19] PsTx blocked olfactory CNG channel (CNGA2) currents with a 30-fold higher affinity than Pdc, and blocked the rod-type channel (CNGA1) with a 15-fold higher affinity, although only seven residues differ between PsTx and Pdc.[3] These residues are critical for binding to the CNG channel, and therefore are plotted on surface model of the triflin. It is interesting that most of these residues are concentrated on the concave surface (Figure 4).

In the process of smooth muscle contraction by depolarization, the concentration of cellular Ca ions mainly depends on the influx of $Ca^{2+}$ through the L-type $Ca^{2+}$ channel.[26–28] In a previous study, we showed that triflin and its homologous proteins (ablomin and latisemin) block depolarization-induced rat tail arterial smooth muscle contraction.[16] These results strongly indicate that those proteins inhibit the influx of $Ca^{2+}$ through the L-type $Ca^{2+}$ channel. A comparison of their activities and sequences revealed that Glu186 and Phe189 (triflin sequence) were most likely to be the functional residues,[2] and these residues also reside on the concave surface (Figures 4 and 5). The ω-conotoxin TxVII protein was isolated from the venom of the molluscivourus marine snail *Conus textile*, and blocks dihydropyridine-sensitive L-type $Ca^{2+}$ channels.[29] This study showed that hydrophobic residues are essential for the peptide-L-type $Ca^{2+}$ channel blockers, like the well-known low molecular mass inhibitors. The hydrophobic residue patches of ω-conotoxin TxVII probably interact with the hydrophobic cluster of the α1 subunit of the L-type $Ca^{2+}$ channel, which consists of 13 residues located within segments 5 and 6 of

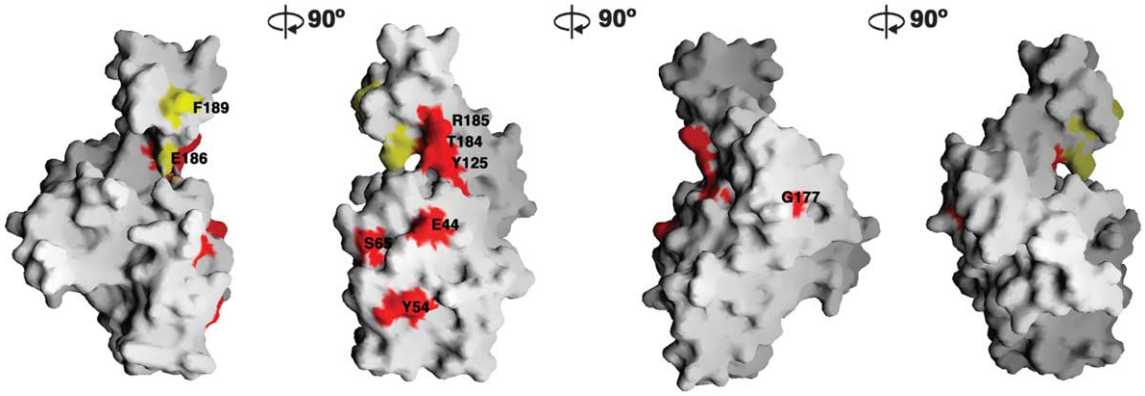


**Figure 4.** Surface models of triflin and putative receptor binding residues. Each model is viewed from a different direction rotated 90° around the vertical axis relative to the neighboring model. The residues that differ between PsTx and Pdc are shown in red with labels. Glu186 and Phe189 are shown in yellow.

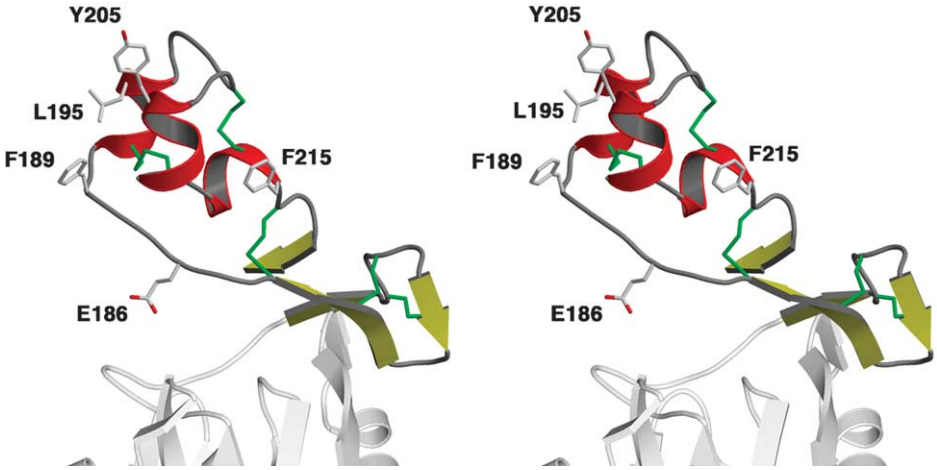


**Figure 5.** Stereo view of the cysteine-rich domain of triflin. The α-helices and β-strands are red and yellow, respectively. Disulfide bonds are shown in green. Hydrophobic residues that are exposed to the solvent are depicted by stick models.

domain III and within segment 6 of domain IV. Similarly, the exposed hydrophobic residues in ω-conotoxin GVIA, which inhibits the N-type $Ca^{2+}$ channel,[30] are also proposed as the functional site, as in the case of TxVII. Therefore, these hydrophobic residues within the cysteine-rich domain of triflin are also good candidates for mediating the interactions between the target proteins. In addition to Phe189 mentioned above, other hydrophobic residues (Leu195, Tyr205 and Phe215) are well conserved and exposed in the vicinity of the apex of the cysteine-rich domain, near the concave surface (Figure 5). However, further investigations (e.g. mutagenesis experiments) are required to determine the responsible residues for the channel inhibition.

After submission of our manuscript, another group have reported the crystal structure of a snake venom CRISP, named Stecrisp, from the venom of *Trimeresurus stejnegeri*.[31] Stecrisp is a highly homologous toxin to triflin with an 87.8% sequence identity, although there is no evidence for its biological activity. In their report, they have shown that the cysteine-rich region of Stecrisp has a similar tertiary structure to voltage-gated potassium channel blockers, BgK and ShK, derived from sea anemones. Structural comparison displays a highly conserved feature of cysteine residues between these blockers and the C-terminal portion of the cysteine-rich region of CRISPs. Several studies on toxins—target channels interaction show that these toxins bind to the selectivity filter and the vestibule of channels rather than pore turret region.[32,33] Corresponding residues to the interaction sites of toxins (Phe6, Lys25, and Tyr26 of BgK) are located near the C-terminal end of the cysteine-rich region (Asn187, Tyr205, and Met206 of triflin) compared with our proposed possible interaction site (residues 184–189 in triflin). These differences strongly suggest a similar but markedly distinct interaction manner between these anemone toxins and snake venom CRISPs on ion channels.

Consequently, the concave surface is likely to be the site that contacts the target ion channel. Particularly, the hydrophobic residues on the concave surface are the candidates for the interactions. The cysteine-rich domain itself could have the binding activity and function as the ion channel blocker. However, we expect that both the specificity and affinity for the target receptor could be increased in cooperation with the PR-1 domain. A number of CRISP family proteins from snake venom have been found, but in most cases their actual functions are unknown. We expect that they may function as various ion-channel blockers, and that the sequence on the concave surface is related to the recognition of the target ion-channel. Moreover, the opening and closing of the concave surface may serve an important role in the induced fitting upon binding.

## Materials and Methods

### Purification and crystallization of trifling

Triflin was purified from the venom of *Trimeresurus flavoviridis*, as described,[16] and was crystallized by mixing 1 μl of a 10 mg/ml triflin solution and 1 μl of reservoir solution at 20 °C, using the hanging-drop vapor-diffusion method. The reservoir solution contained 100 mM Tris–HCl (pH 8.0), 1.0 M sodium acetate, 200 mM $CdCl_2$, and 1.5% (w/v) polyethylene glycol 400.The crystals grew to a typical size of 0.3 mm×0.2 mm×0.2 mm, and were subjected to X-ray data collection. The crystals belong to the tetragonal space group $P4_32_12$, with $a=b=83.3$ Å, $c=85.7$ Å. There is one molecule in the asymmetric unit based on the Matthews coefficient calculation ($V_M=3.1$ Å$^3$/Da),[34] resulting in a solvent content of 60%.

### Data collection and structure determination

Crystals were harvested into a cryoprotectant solution, composed of reservoir solution containing 30% (v/v) glycerol, and were flash frozen in a stream of $N_2$ gas at

100 K. Potential heavy-atom derivatives were investigated with a heavy-atom screen kit (Hampton Research). After identifying $HAuCl_4$ as a promising candidate for derivatization, the triflin crystals were soaked in 2 mM $HAuCl_4$ for 28 hours. All diffraction data were collected on a marCCD165 detector (Mar Inc.), using synchrotron radiation at beamline BL41XU of SPring-8.Three-wavelength anomalous data sets were collected on a single gold derivative (L-III edge) crystal, and a one-wavelength data set was obtained with a native crystal. Data processing was performed using the program MOSFLM.[35] Data scaling and merging were performed using the CCP4 package.[35] Two gold sites were confirmed in the anomalous difference map from the peak wavelength of the gold derivative. Initial multi-wavelength anomalous diffraction (MAD) phases were calculated with SHARP[36] and were subsequently improved by density modification with DM.[35] The model building and manual fitting were performed with QUANTA (Molecular Simulations, Waltham, MA). The initial model was refined against the peak wavelength data set, using simulated annealing algorithms, by the program CNS.[37] Due to the good isomorphism between the gold derivative and native data sets, the refinement against the native data was performed after the rigid body refinement. This model was further refined by CNS. Data collection, phasing and refinement statistics are given in Table 1.

### Protein Data Bank accession number

The coordinates and the structure factors of triflin have been deposited in the RCSB Protein Data Bank with accession number 1WVR.

## Acknowledgements

We thank members of the staff at beamline BL41XU of SPring-8 for assistance in data collection. This research was supported in part by Scientific Research Grants-in-Aid (T.M.) and by Special Coordination Funds for Promoting Science and Technology (H.M.) from the Ministry of Education, Science, Sports and Culture of Japan.

## References

1. Kierszenbaum, A. L., Lea, O., Petrusz, P., French, F. S. & Tres, L. L. (1981). Isolation, culture, and immunocytochemical characterization of epididymal epithelial cells from pubertal and adult rats. *Proc. Natl Acad. Sci. USA*, **78**, 1675–1679.
2. Charest, N. J., Joseph, D. R., Wilson, E. M. & French, F. S. (1988). Molecular cloning of complementary deoxyribonucleic acid for an androgen-regulated epididymal protein: sequence homology with metalloproteins. *Mol. Endocrinol.* **2**, 999–1004.
3. Ellerman, D. A., Da Ros, V. G., Cohen, D. J., Busso, D., Morgenfeld, M. M. & Cuasnicu, P. S. (2002). Expression and structure–function analysis of de, a sperm cysteine-rich secretory protein that mediates gamete fusion. *Biol. Reprod.* **67**, 1225–1231.
4. Kasahara, M., Gutknecht, J., Brew, K., Spurr, N., Goodfellow, P. N., Passmore, H. C. & Klein, J. (1989). Cloning and mapping of a testis-specific gene with sequence similarity to a sperm-coating glycoprotein gene. A testis-specific gene Tpx-1 maps between Pgk-2 and Mep-1 on mouse chromosome 17. *Genomics*, **5**, 527–534.
5. Kjeldsen, L., Cowland, J. B., Johnsen, A. H. & Borregaard, N. (1996). SGP28, a novel matrix glycoprotein in specific granules of human neutrophils with similarity to a human testis-specific gene product and a rodent sperm-coating glycoprotein. *FEBS Letters*, **380**, 246–250.
6. Mochca-Morales, J., Martin, B. M. & Possani, L. D. (1990). Isolation and characterization of helothermine, a novel toxin from *Heloderma horridum horridum* (Mexican beaded lizard) venom. *Toxicon*, **28**, 299–309.
7. Morrissette, J., Kratzschmar, J., Haendler, B., el-Hayek, R., Mochca-Morales, J., Martin, B. M. *et al*. (1995). Primary structure and properties of helothermine, a peptide toxin that blocks ryanodine receptors. *Biophys. J.* **68**, 2280–2288.
8. Nobile, M., Magnelli, V., Lagostena, L., Mochca-Morales, J., Possani, L. D. & Prestipino, G. (1994). The toxin helothermine affects potassium currents in newborn rat cerebellar granule cells. *J. Membr. Biol.* **139**, 49–55.
9. Nobile, M., Noceti, F., Prestipino, G. & Possani, L. D. (1996). Helothermine, a lizard venom toxin, inhibits calcium current in cerebellar granules. *Expt. Brain Res.* **110**, 15–20.
10. Olson, J. H., Xiang, X., Ziegert, T., Kittelson, A., Rawls, A., Bieber, A. L. & Chandler, D. E. (2001). Allurin, a 21-kDa sperm chemoattractant from *Xenopus* egg jelly, is related to mammalian sperm-binding proteins. *Proc. Natl Acad. Sci. USA*, **98**, 11205–11210.
11. Ookuma, S., Fukuda, M. & Nishida, E. (2003). Identification of a DAF-16 transcriptional target gene, scl-1, that regulates longevity and stress resistance in *Caenorhabditis elegans*. *Curr. Biol.* **13**, 427–431.
12. Fernandez, C., Szyperski, T., Bruyere, T., Ramage, P., Mosinger, E. & Wuthrich, K. (1997). NMR solution structure of the pathogenesis-related protein P14a. *J. Mol. Biol.* **266**, 576–593.
13. Henriksen, A., King, T. P., Mirza, O., Monsalve, R. I., Meno, K., Ipsen, H. *et al*. (2001). Major venom allergen of yellow jackets. Ves v 5: structural characterization of a pathogenesis-related protein superfamily. *Proteins: Struct. Funct. Genet.* **45**, 438–448.
14. Yamazaki, Y. & Morita, T. (2004). Structure and function of snake venom cysteine-rich secretory proteins. *Toxicon*, **44**, 227–231.
15. Yamazaki, Y., Hyodo, F. & Morita, T. (2003). Wide distribution of cysteine-rich secretory proteins in snake venoms: isolation and cloning of novel snake venom cysteine-rich secretory proteins. *Arch. Biochem. Biophys.* **412**, 133–141.
16. Yamazaki, Y., Koike, H., Sugiyama, Y., Motoyoshi, K., Wada, T., Hishinuma, S. *et al*. (2002). Cloning and characterization of novel snake venom proteins that block smooth muscle contraction. *Eur. J. Biochem.* **269**, 2708–2715.
17. Brown, R. L., Haley, T. L., West, K. A. & Crabb, J. W. (1999). Pseudechetoxin: a peptide blocker of cyclic nucleotide-gated ion channels. *Proc. Natl Acad. Sci. USA*, **96**, 754–759.
18. Yamazaki, Y., Brown, R. L. & Morita, T. (2002). Purification and cloning of toxins from elapid venoms that target cyclic nucleotide-gated ion channels. *Biochemistry*, **41**, 11331–11337.

19. Brown, R. L., Lynch, L. L., Haley, T. L. & Arsanjani, R. (2003). Pseudechetoxin binds to the pore turret of cyclic nucleotide-gated ion channels. *J. Gen. Physiol.* **122**, 749–760.
20. Takahashi, H., Kim, J. I., Min, H. J., Sato, K., Swartz, K. J. & Shimada, I. (2000). Solution structure of hanatoxin1, a gating modifier of voltage-dependent K(+) channels: common surface features of gating modifier toxins. *J. Mol. Biol.* **297**, 771–780.
21. Lee, C. W., Kim, S., Roh, S. H., Endoh, H., Kodera, Y., Maeda, T. *et al*. (2004). Solution structure and functional characterization of SGTx1, a modifier of Kv2.1 channel gating. *Biochemistry*, **43**, 890–897.
22. Lee, S. Y. & MacKinnon, R. (2004). A membrane-access mechanism of ion channel inhibition by voltage sensor toxins from spider venom. *Nature*, **430**, 232–235.
23. Gerstein, M., Lesk, A. M. & Chothia, C. (1994). Structural mechanisms for domain movements in proteins. *Biochemistry*, **33**, 6739–6749.
24. Szyperski, T., Fernandez, C., Mumenthaler, C. & Wuthrich, K. (1998). Structure comparison of human glioma pathogenesis-related protein GliPR and the plant pathogenesis-related protein P14a indicates a functional link between the human immune system and a plant defense system. *Proc. Natl Acad. Sci. USA*, **95**, 2262–2266.
25. Milne, T. J., Abbenante, G., Tyndall, J. D., Halliday, J. & Lewis, R. J. (2003). Isolation and characterization of a cone snail protease with homology to CRISP proteins of the pathogenesis-related protein superfamily. *J. Biol. Chem.* **278**, 31105–31110.
26. Chen, X. L. & Rembold, C. M. (1995). Phenylephrine contracts rat tail artery by one electromechanical and three pharmacomechanical mechanisms. *Am. J. Physiol.* **268**, H74–H81.
27. Bolton, T. B., Prestwich, S. A., Zholos, A. V. & Gordienko, D. V. (1999). Excitation-contraction coupling in gastrointestinal and other smooth muscles. *Annu. Rev. Physiol.* **61**, 85–115.
28. Mita, M., Yanagihara, H., Hishinuma, S., Saito, M. & Walsh, M. P. (2002). Membrane depolarization-induced contraction of rat caudal arterial smooth muscle involves Rho-associated kinase. *Biochem. J.* **364**, 431–440.
29. Fainzilber, M., Lodder, J. C., van der Schors, R. C., Li, K. W., Yu, Z., Burlingame, A. L. *et al*. (1996). A novel hydrophobic omega-conotoxin blocks molluscan dihydropyridine-sensitive calcium channels. *Biochemistry*, **35**, 8748–8752.
30. Lew, M. J., Flinn, J. P., Pallaghy, P. K., Murphy, R., Whorlow, S. L., Wright, C. E. *et al*. (1997). Structure–function relationships of omega-conotoxin GVIA. Synthesis, structure, calcium channel binding, and functional assay of alanine-substituted analogues. *J. Biol. Chem.* **272**, 12014–12023.
31. Guo, M., Teng, M., Niu, L., Liu, Q., Huang, Q. & Hao, Q. (2005). Crystal structure of the cysteine-rich secretory protein stecrisp reveals that the cysteine-rich domain has a $K^+$ channel inhibitor-like fold. *J. Biol. Chem.* **280**, 12405–12412.
32. Lanigan, M. D., Kalman, K., Lefievre, Y., Pennington, M. W., Chandy, K. G. & Norton, R. S. (2002). Mutating a critical lysine in ShK toxin alters its binding configuration in the pore-vestibule region of the voltage-gated potassium channel, Kv1.3. *Biochemistry*, **41**, 11963–11971.
33. Rauer, H., Pennington, M., Cahalan, M. & Chandy, K. G. (1999). Structural conservation of the pores of calcium-activated and voltage-gated potassium channels determined by a sea anemone toxin. *J. Biol. Chem.* **274**, 21885–21892.
34. Matthews, B. W. (1968). Solvent content of protein crystals. *J. Mol. Biol.* **33**, 491–497.
35. Collaborative Computational Project, N. (1994). The CCP4 suite: programs for protein crystallography. *Acta Crystallog. sect. D*, **50**, 760–763.
36. de La Fortelle, E. & Bricogne, G. (1997). Maximum-likelihood heavy-atom parameter refinement for the multiple isomorphous replacement and multiwavelength anomalous diffraction methods. In *Methods Enzymology* (Carter, J. C. W. & Sweet, R. M., eds), pp. 472–494, Academic Press, New York.
37. Brunger, A. T., Adams, P. D., Clore, G. M., DeLano, W. L., Gros, P., Grosse-Kunstleve, R. W. *et al*. (1998). Crystallography and NMR system: a new software suite for macromolecular structure determination. *Acta Crystallog. sect. D*, **54**, 905–921.

***Edited by R. Huber***

*(Received 7 March 2005; received in revised form 2 May 2005; accepted 11 May 2005)*